



# Cleaning the TESS observations of WASP-33 b transits from the host star photometric variability

R. Baluev<sup>1,2</sup> and E. Sokov<sup>3</sup>

<sup>1</sup> Saint Petersburg State University, 7–9 Universitetskaya nab., St. Petersburg, 199034 Russia

<sup>2</sup> Special Astrophysical Observatory of the Russian Academy of Sciences,  
Nizhny Arkhyz, 369167 Russia

<sup>3</sup> Central Astronomical Observatory at Pulkovo, Russian Academy of Sciences,  
65/1 Pulkovskoje sh., St. Petersburg, 196140 Russia

**Abstract.** Based on the TESS observations of a  $\delta$  Scuti variable WASP-33 obtained in 2019 and 2022, we thoroughly investigate the power spectrum of its photometric flux and construct a statistically exhaustive model for its variation. This model contains 30 robustly justified harmonics, the red noise, and quasiperiodic noise components. This compound model allows us to greatly improve the transit timing accuracy of the exoplanet WASP-33 b. The rms of its transit timing variation residuals is drastically reduced by a factor of 3.5, from 63 s to 18 s.

**Keywords:** techniques: photometric; stars: variables: delta Scuti; stars: individual: WASP-33; planets and satellites: detection

**DOI:** 10.26119/VAK2024.128

# 1 Introduction

WASP-33 (HD 15082) is a bright  $8^m14$  fast-rotating star with  $v \sin i \sim 90$  km/s, located in Andromeda. Its the only known exoplanet WASP-33 b was detected by SuperWASP (Herrero et al. 2011). Its orbital period is estimated as  $1.219867 \pm 4.2 \cdot 10^{-5}$  d (von Essen et al. 2020), the mass as  $2.10 \pm 0.14 M_{\text{Jup}}$ , and the radius as  $1.59 \pm 0.07 R_{\text{Jup}}$  (Chakrabarty & Sengupta 2019). Remarkably, this exoplanet was the first ever known to orbit a  $\delta$  Scuti variable.

The intrinsic variability of WASP-33 represents an obvious nuisance factor for analysing the transit light curves of its exoplanet WASP-33 b. The effect of this variability on the estimated planetary orbital parameters was previously investigated using out-of-transit observations from ground-based telescopes located in Germany and Spain (von Essen et al. 2014). Eight significant pulsation frequencies were revealed, and it was concluded that cleaning the transit light curves from stellar pulsations does not practically affect the estimated planetary parameters, though their uncertainties had decreased. Besides, it was noticed that WASP-33 pulsation phases change over time. In a later analysis of the TESS data of 2019, von Essen et al. (2020) expanded the number of pulsation harmonics to 29. They also claimed the detection of the exoplanet secondary eclipse, its phase curve variation, and the “ellipsoidal variation” appearing because of the subtle exoplanet gravitation effect on the host star shape.

Our goal here is to analyse WASP-33 pulsations based on the up-to-date TESS data (observations in 2019 and 2022) and to investigate whether (and how much) this can help us improve the transit timings accuracy for this target.

## 2 TESS photometry of WASP-33

TESS observed WASP-33 in sector 18 (Nov 2019) and sector 58 (Nov 2022), lasting about 1 month each. In the data validation time series downloaded from the Mikulski Archive for Space Telescopes,<sup>4</sup> we found 14 796 and 18 951 photometric measurements for these sectors, respectively. We also identified 17 transits in sector 18 and 21 transits in sector 58, and for each transit we extracted a  $\pm 4$  h piece of the light curve around the predicted mid-transit epoch. This subset formed our first “in-transit” dataset (ITD). The second “out-of-transit” dataset (OTD) included all the observations located at least  $\pm 2$  h away from the centers of the transits or secondary eclipses. Note that the ITD and OTD slightly overlap.

---

<sup>4</sup> <https://archive.stsci.edu/>

In this work we deal mainly with the OTD. Its sector 18 portion is hereafter referred to as TESS<sub>1</sub>, and it contains 10 684 data points. The sector 58 portion (TESS<sub>2</sub>) contains 13 625 data points. The ITD contains 8914 data points in total.

### 3 Statistically exhaustive model of WASP-33 variability

Our goal was to construct a statistically “exhaustive” model that represents the WASP-33 data in such a way that the residuals do not contain statistically significant periodic (or quasiperiodic) variations. In this attempt we adopted a sum of sinusoids for the deterministic part of the model:

$$\mu_n(t) = A_0 + \sum_{k=1}^n A_k \cos(2\pi f_k(t - T_0) + \varphi_k), \quad (1)$$

where  $A_k$ ,  $f_k = 1/P_k$ , and  $\varphi_k$  are free parameters. However, the photometric variation involves significant non-deterministic part with a multiband power spectrum. It cannot be efficiently modeled by deterministic models like (1) because we would need too many terms (hundreds in our case). Such quasiperiodic variations are much better treated as a non-white noise (NWN), which offers a great reduction in the number of free parameters. Using this approach, we model the NWN correlation function:

$$k_{n'}(\Delta t_{ij}) = (\sigma_{\text{TESS},i}^2 + \sigma_0^2) \delta_{ij} + \sum_{k=1}^{n'} \sigma_k^2 e^{-\frac{|\Delta t_{ij}|}{\tau_k}} \cos 2\pi f'_k \Delta t_{ij}, \quad \Delta t_{ij} = t_i - t_j, \quad (2)$$

where  $\sigma_{\text{TESS},i}$  is the TESS-provided photometric uncertainty at  $t_i$ ,  $\delta_{ij}$  is the Kronecker delta, and the remaining quantities ( $\sigma_k$ ,  $\tau_k$ ,  $f'_k = 1/P'_k$ ) are free parameters. This model involves the white noise (WN) portion ( $\sigma_0$ ) and  $n'$  independent quasiperiodic (QP) components (purely NWN part). Models (1) and (2) can be fitted jointly by the maximum-likelihood method if we assume that the NWN is a random Gaussian process (GP) which implies a multivariate Gaussian distribution for the data vector.

Details of the subsequent periodogram analysis, including the statistical testing of the harmonics, are too lengthy and will be presented in another paper. We applied our algorithm separately to the TESS 2019 and 2022 observing runs, and both these datasets revealed very similar sets of harmonics. In Fig. 1 we plot all the detected harmonics in the frequency–amplitude plane (with uncertainties). Harmonics that were cross-identified by their frequencies are additionally labeled with circles. Nearly all the harmonics, namely 30 of them, can be robustly cross-identified by their frequencies. Usually, the amplitudes of the cross-identified harmonics are similar, although

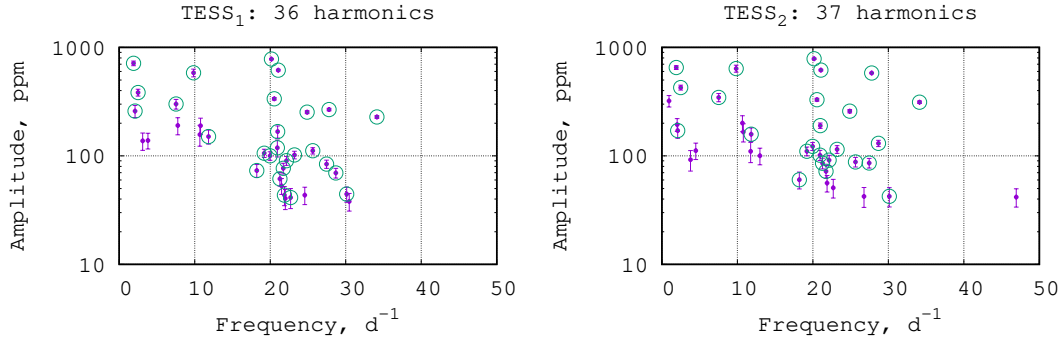


**Fig. 1.** All the detected harmonics in the frequency–amplitude plane.

some of them have demonstrated a large change between the 2019 and 2022 runs. One may conclude that the WASP-33 variability pattern demonstrates remarkable, though not entirely perfect, stability on the timescale of a few years at least.

Table 1 contains the best-fit NWN parameters of the GP kernel (Eq. 2). It contains the mandatory WN term, one red noise (RN) term with a period  $P'_1$  much larger than  $\tau_1$ , and one QP term with  $P'_2$  smaller than but comparable to  $\tau_2$ . The second NWN term appears nearly the same for the 2019 and 2022 datasets, although the WN and RN parts reveal significant changes.

**Table 1.** Estimated GP parameters.

	$\sigma_0$ , ppm	$\sigma_1$ , ppm	$\tau_1$ , d	$P'_1$ , d	$\sigma_2$ , ppm	$\tau_2$ , d	$P'_2$ , d
TESS <sub>1</sub>	260.4(5.3)	525(47)	0.52(13)	1.65(23)	426(23)	0.182(26)	0.1085(15)
TESS <sub>2</sub>	544.6(4.9)	294(23)	0.23(98)	$\infty$ ( $\gtrsim 1.7$ )	470(22)	0.182(21)	0.1084(13)

## 4 Improving transit timing accuracy

Now let us consider how our out-of-transit photometric model of WASP-33 can be used to detrend the transit light curves. Our model contains two components: the deterministic one  $\mu(t)$  (harmonics) and the GP part (NWN) expressed by the correlation function  $k(\Delta t)$ . Regarding the former, we can subtract the best fitting  $\mu(t)$  from the ITD as if it was a predefined function: it has very small uncertainty because the number of the OTD data from which it has been derived is much larger than that of the ITD. We will call this “detrending” for shortness.

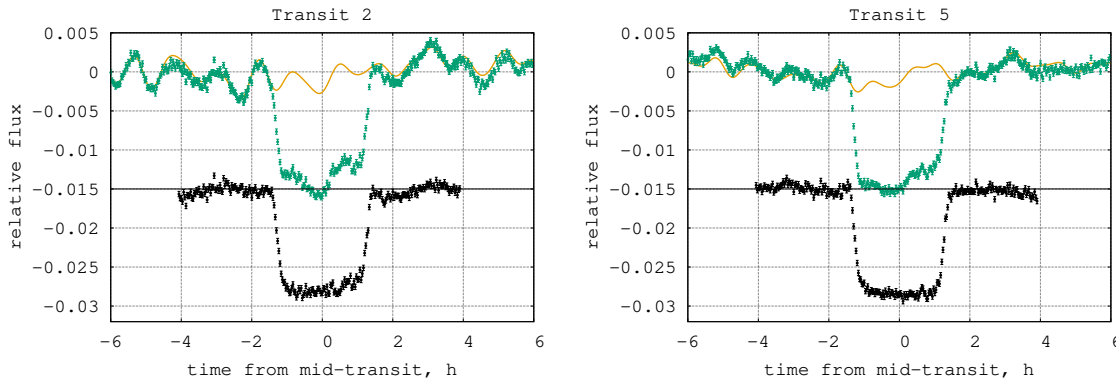


**Fig. 2.** Detrending examples for WASP-33 b transits 2 and 5.

Regarding the NWN part of the model, its effect can be removed by applying the whitening procedure to the ITD and the NWN model simultaneously, using the covariance matrix derived from the best-fit  $k(\Delta t)$ . It is unnecessary to apply this procedure in an explicit way, and in fact it is automatically (but implicitly) applied in our NWN analysis that relies on the maximum-likelihood GP fitting. However, we will call this part of the processing as “whitening” for simplicity.

In Fig. 2 we show examples of detrending for two transits of WASP-33 b. In the figure we plot the TESS data before processing (green points), the harmonics model  $\mu$  (orange curve), and the detrended ITD (black points, shifted down). One can see that detrending can remove a large portion of the host star variability; however, some nuisance variation still remains. Obviously, this variation appears because of the NWN and should be removed by whitening.

Since our whitening is implicit, we do not show any whitened data in Fig. 2. However, its effect is demonstrated in Fig. 3, where we plot the resulting transit timing residuals derived from (1) the initial (raw) ITD, (2) detrended ITD, and (3) detrended and whitened ITD. One can see that the transit timing variation (TTV) scatter remarkably reduces after each step: while the rms of the initial TTV residuals was 63 s, the detrending reduced it to 36 s, and after the whitening it dropped to 18 s. The final set of these improved transit timings will be published in another paper.

## 5 Conclusions

An approach based on the explicit modeling of WASP-33 variability appears extremely successful in improving its exoplanet transit timing accuracy. In total, we

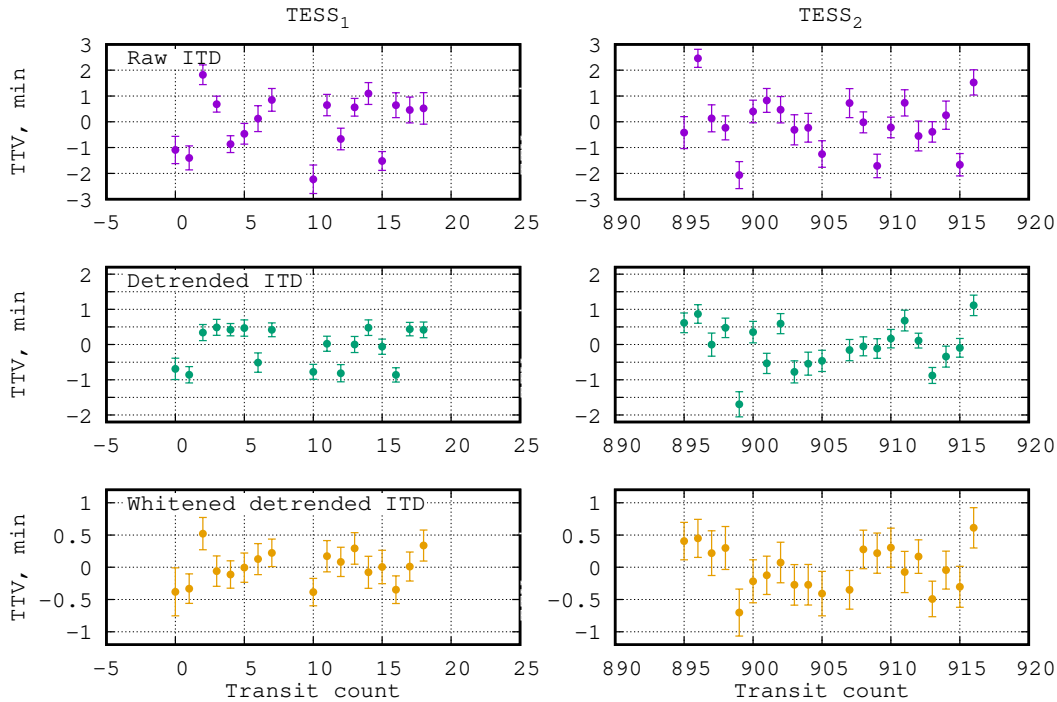


**Fig. 3.** WASP-33 transit timing residuals before and after ITD cleaning. Note the different ordinate ranges in the plots.

obtained a dramatic TTV rms improvement by a factor of 3.5. It is important that we take into account the deterministic as well as non-deterministic (NWN) parts of this variability. Both of them incorporate similar amounts into the total error budget.

Our results still cannot be directly applied to observations other than from TESS because the model parameters somewhat change on the timescale of a few years. Because of that, we cannot use the TESS-derived model with data obtained, e.g., years prior to TESS. However, the frequencies of the harmonics and of the QP part of the NWN look stable, so it may be possible to apply our model to older data, fixing all these frequencies but refitting harmonics amplitudes and phases as well as the variances of the NWN components. This needs additional investigation.

## References

- Chakrabarty A. and Sengupta S., 2019, *Astronomical Journal*, 158, p. 39  
 Herrero E., Morales J.C., Ribas I., et al., 2011, *Astronomy and Astrophysics*, 526, L10  
 von Essen C., Czesla S., Wolter U., et al., 2014, *Astronomy and Astrophysics*, 561, A48  
 von Essen C., Mallonn M., Borre C.C., et al., 2020, *Astronomy and Astrophysics*, 639, A34